DALTON
FULL PAPER

Ruthenium-mediated reduction of oximes to imines. Synthesis, characterization and redox properties of imine complexes of ruthenium

Anjan Kumar Das,[a] Shie-Ming Peng[b] and Samaresh Bhattacharya *[a]

[a] *Department of Chemistry, Inorganic Chemistry Section, Jadavpur University, Calcutta 700 032, India*
[b] *Department of Chemistry, National Taiwan University, Taipei, Taiwan, Republic of China*

Received 31st August 1999, Accepted 15th November 1999

Reaction of three oxime ligands (oximes of salicylaldehyde (HL^1–O), 2-hydroxyacetophenone (HL^2–O) and 2-hydroxynaphthylaldehyde (HL^3–O); where H stands for the phenolic proton and O for the oxime oxygen) with $[Ru(PPh_3)_3Cl_2]$ in a 1 : 1 molar ratio brings about reduction of the oximes to imines and affords complexes of the form $[Ru(PPh_3)_2(L)Cl_2]$, where L stands for the deprotonated imine ligand which is coordinated as a *N*,*O*-donor forming a six-membered chelate ring. The structure of the $[Ru(PPh_3)_2(L^2)Cl_2]$ complex has been solved by X-ray crystallography. The coordination sphere around ruthenium is composed of NOP_2Cl_2 with the two PPh_3 ligands in mutually *trans* and the two chlorides in mutually *cis* positions. The $[Ru(PPh_3)_2(L)Cl_2]$ complexes are one-electron paramagnetic (low-spin d^5, $S = 1/2$) and show rhombic EPR spectra in 1 : 1 dichloromethane–toluene solution at 77 K. In dichloromethane solution the $[Ru(PPh_3)_2(L)Cl_2]$ complexes show several intense LMCT transitions in the visible region, together with a weak ligand field transition near 1700 nm. Cyclic voltammetry on the $[Ru(PPh_3)_2(L)Cl_2]$ complexes shows a ruthenium(III)–ruthenium(II) reduction near −0.4 V *vs*. SCE and a ruthenium(III)–ruthenium(IV) oxidation in the range 0.88–1.15 V *vs*. SCE.

Introduction

Metal-promoted chemical transformation of organic molecules has been of significant current interest.[1] Herein we wish to disclose an example of ruthenium-mediated reduction of oximes to imines (eqn. 1). It may be noted here that such reduction of oximes to imines appears to be unusual. The ligands used in the present study are oximes of salicylaldehyde, 2-hydroxyacetophenone and 2-hydroxynaphthaldehyde. All these ligands are abbreviated in general as HL–O, where H stands for the dissociable phenolic proton and O for the oxime oxygen. Individual abbreviations are shown with structure **1**. The ruthenium complex utilized for bringing about reduction of these oximes was $[Ru(PPh_3)_3Cl_2]$. Reaction of the oximes with $[Ru(PPh_3)_3Cl_2]$ afforded a group of complexes of the type $[Ru(PPh_3)_2(L)Cl_2]$, where L stands for the deprotonated imine ligand. The chemistry of these complexes is described here with special reference to synthesis, characterization and redox properties.

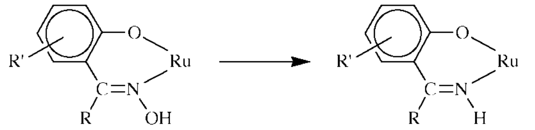

(1)

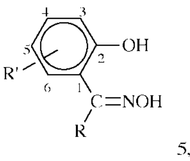

R'	R	Ligand
H	H	HL^1-O
H	CH_3	HL^2-O
5,6-benzo	H	HL^3-O

1

Experimental

Materials

$[Ru(PPh_3)_3Cl_2]$ was synthesized by following a literature method.[2] The oximes were prepared by reacting equimolar amounts of the respective aldehydes and hydroxylamine, following a reported procedure.[3] Purification of dichloromethane and preparation of tetrabutylammonium perchlorate (TBAP) for electrochemical work was carried out as reported in the literature.[4]

Preparations

$[Ru(PPh_3)_2(L^1)Cl_2]$. $[Ru(PPh_3)_3Cl_2]$ (100 mg, 0.10 mmol) was refluxed with salicylaldoxime (16 mg, 0.11 mmol) in ethanol (50 cm^3) for 2 h. A green microcrystalline precipitate of $[Ru(PPh_3)_2(L^1)Cl_2]$ started to separate out during the reflux. After cooling the solution to room temperature, the precipitate was collected by filtration, washed with ethanol and dried in air. Recrystallization from 1 : 4 dichloromethane–hexane gave $[Ru(PPh_3)_2(L^1)Cl_2]$ as a green crystalline solid in 72% yield. Anal. Calc. for $C_{43}H_{35}NOCl_2P_2Ru$: C, 63.23; H, 4.41; N, 1.72. Found: C, 63.30; H, 4.45; N, 1.73%.

$[Ru(PPh_3)_2(L^2)Cl_2]$. This complex was prepared by following the same procedure as above, using the oxime of 2-hydroxyacetophenone (HL^2–O) instead of salicylaldoxime. The yield was 70%. Anal. Calc. for $C_{44}H_{38}NOCl_2P_2Ru$: C, 63.61; H, 4.58; N, 1.69. Found: C, 63.66; H, 4.61; N, 1.70%.

$[Ru(PPh_3)_2(L^3)Cl_2]$. This complex was prepared by following the same synthetic procedure as for $[Ru(PPh_3)_2(L^1)Cl_2]$, using the oxime of 2-hydroxynaphthaldehyde (HL^3–O) instead of salicylaldoxime. The yield was 70%. Anal. Calc. for $C_{47}H_{37}NOCl_2P_2Ru$: C, 64.8; H, 4.25; N, 1.60. Found: C, 64.24; H, 4.68; N, 1.69%.

Physical measurements

Microanalyses (C, H, N) were performed using a Perkin-Elmer 240C elemental analyzer. IR spectra were obtained on a Perkin-Elmer 783 spectrometer with samples prepared as KBr pellets. Electronic spectra were recorded on a Shimadzu UV 240 spectrophotometer. Magnetic susceptibilities were measured

Table 1 Crystallographic data for $[Ru(PPh_3)_2(L^2)Cl_2]$

Empirical formula	$C_{44}H_{38}NOP_2Cl_2Ru$
f_w	830.7
Space group	Monoclinic, $P2_1/n$
a/Å	9.471(3)
b/Å	23.981(3)
c/Å	17.290(5)
β/°	97.23(3)
V/Å^3	3895.8(17)
Z	4
Crystal size/mm	0.50 × 0.50 × 0.50
T/°C	25
μ/cm^{-1}	6.471
R_f	0.026^a
R_w	0.028^b
GOF	2.75^c

^{a} $R_f = \Sigma||F_o| - |F_c||/\Sigma|F_o|$. ^{b} $R_w = [\Sigma w(|F_o| - |F_c|)^2/\Sigma w(F_o)^2]^{\frac{1}{2}}$. ^{c} GOF = $[\Sigma w(|F_o| - |F_c|)^2/(M - N)]^{\frac{1}{2}}$, where M is the number of reflections and N is the number of parameters refined.

Table 2 Selected bond distances and bond angles for $[Ru(PPh_3)_2(L^2)Cl_2]$

Bond distances/Å		Bond angles/°	
Ru–Cl1	2.3696(10)	P1–Ru–P2	178.319(21)
Ru–Cl2	2.3718(9)	Cl2–Ru–N1	174.53(6)
Ru–P1	2.4242(7)	Cl1–Ru–O1	172.34(5)
Ru–P2	2.4176(8)	Cl1–Ru–Cl2	98.92(4)
Ru–O1	1.9687(15)	O1–Ru–N1	86.36(7)
Ru–N1	2.0225(19)		
O1–C1	1.319(3)		
N1–C7	1.298(3)		

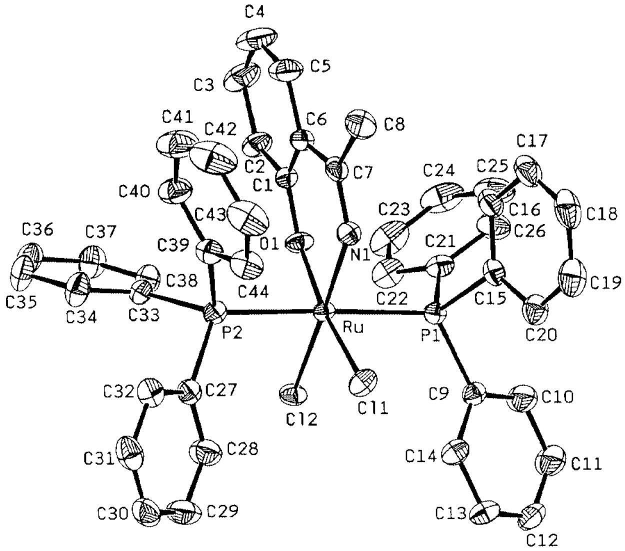

Fig. 1 View of the $[Ru(PPh_3)_2(L^2)Cl_2]$ molecule.

using a PAR 155 vibrating sample magnetometer. EPR spectra were recorded on a Varian Model 109C E-line X-band spectrometer fitted with a quartz Dewar for measurements at 77 K (liquid dinitrogen). All spectra were calibrated against the spectrum of DPPH ($g = 2.0037$). Electrochemical measurements were made using a PAR model 273 potentiostat. A platinum disc or graphite working electrode, a platinum wire auxiliary electrode and an aqueous saturated calomel reference electrode (SCE) were used in a three-electrode configuration. An RE 0089 X-Y recorder was used to trace the voltammograms. Electrochemical measurements were made under a dinitrogen atmosphere. All electrochemical data were collected at 298 K and are uncorrected for junction potentials.

Crystallography

Single crystals of $[Ru(PPh_3)_2(L^2)Cl_2]$ were grown by slow diffusion of hexane into a dichloromethane solution of the complex. Selected crystal data and data collection parameters are given in Table 1. Data were collected on an Enraf-Nonius CAD-4 diffractometer using graphite-monochromated Mo-Kα radiation ($\lambda = 0.71073$ Å). Three standard reflections measured every 3600 s of X-ray exposure showed no significant intensity variation over the course of data collection. X-Ray data reduction and structure solution and refinement were carried out using the NRCVAX package.[5]

CCDC reference number 186/1739.

See http://www.rsc.org/suppdata/dt/a9/a907021d/ for crystallographic files in .cif format.

Results and discussion

Reaction of the oximes (HL–O) with $[Ru(PPh_3)_3Cl_2]$ proceeded smoothly in refluxing ethanol to afford imine complexes of the type $[Ru(PPh_3)_2(L)Cl_2]$ in good yields. Formation of the imine complexes has been authenticated by structural characterization of $[Ru(PPh_3)_2(L^2)Cl_2]$. The structure is shown in Fig. 1 and selected bond parameters are listed in Table 2. The oxime of 2-hydroxyacetophenone has lost the oxime oxygen and the resulting imine ligand is coordinated to ruthenium as a bidentate *N*,*O*-donor ligand, forming a six-membered chelate ring with a bite angle of 86.36°. The two PPh_3 ligands are mutually *trans*, as is usually observed in complexes of ruthenium(III) containing the $Ru(PPh_3)_2$ moiety,[6] and the two chloride ligands occupy mutually *cis* positions. The NOP_2Cl_2 coordination sphere around ruthenium is distorted octahedral in nature. The Ru–N, Ru–O, Ru–P and Ru–Cl bond lengths are all quite unremarkable, as are the phenolic C–O and imine C–N distances.[7] In view of the observed similarity in spectral and electrochemical properties (*vide infra*), the other two $[Ru(PPh_3)_2(L)Cl_2]$ complexes are assumed to have a similar structure. The mechanism of this reaction is not yet clear. However, an oxygen from the oxime ligand is probably transferred to a PPh_3,, dissociated from $[Ru(PPh_3)_3Cl_2]$. Indirect evidence for this oxo-transfer comes from detection of $OPPh_3$ in the residue of the synthetic reactions (after isolation of $[Ru(PPh_3)_2(L)Cl_2]$), identified by its characteristic infrared spectrum ($\nu_{P\text{–}O}$ observed at 1185 cm^{-1}). Triphenylphosphine is well known to act as an oxygen-scavenger in many oxo-transfer reactions.[8] The role of $[Ru(PPh_3)_3Cl_2]$ in this reaction is not yet clear, but that it does not act as a mere supplier of PPh_3 is clear from the fact that a mixture of PPh_3 and the oxime is unable to bring about an oxo-transfer reaction. Prior coordination of the oxime ligand to ruthenium, followed by oxo-transfer from the metal-bound ligand appears probable.

Infrared spectra of the $[Ru(PPh_3)_2(L)Cl_2]$ complexes show strong vibrations near 520, 695 and 740 cm^{-1}, which are attributed to the $Ru(PPh_3)_2$ fragment.[9] A sharp peak near 3300 cm^{-1} is consistent with the presence of an N–H bond[10] in the coordinated imine fragment of the phenolate ligands. Two ν(Ru–Cl) stretches are observed near 330 and 320 cm^{-1} due to the *cis*-$RuCl_2$ fragment.[11] The $[Ru(PPh_3)_2(L)Cl_2]$ complexes are soluble in polar organic solvents, such as dichloromethane, chloroform, acetonitrile, *etc.*, producing intense green solutions. The electronic spectra of these complexes have been recorded in dichloromethane solution. Spectral data are presented in Table 3 and a representative UV-vis spectrum is shown in Fig. 2. Each complex shows a few very intense absorptions in the ultraviolet region, several intense absorptions in the visible region and a weak absorption in the near-IR region. The absorptions in the ultraviolet region are attributable to transitions occurring within the ligand orbitals. The intense absorptions observed in the visible region may be assigned to ligand-to-metal charge-transfer

Table 3 Electronic spectral and cyclic voltammetric data

Compound	μ_{eff}/μ_B	Electronic spectral data[a] λ_{max}/nm (ε/M^{-1} cm^{-1})	Cyclic voltammetric data[a,b] $E_{1/2}$/V (ΔE_p/mV)	
			Ru^{III}–Ru^{IV}	Ru^{III}–Ru^{II}
[Ru(PPh$_3$)$_2$(L^1)Cl$_2$]	1.86	1745 (21), 685 (2200), 360[c] (9300), 298 (26100)	1.15 (70)	−0.38[d]
[Ru(PPh$_3$)$_2$(L^2)Cl$_2$]	1.91	1670 (28), 672 (1800), 350[c] (8100), 297 (23200)	0.88 (70)	−0.41[d]
[Ru(PPh$_3$)$_2$(L^3)Cl$_2$]	1.93	1740 (34), 710 (2300), 367[c] (10000), 300 (26600)	0.90 (70)	−0.36[d]

[a] In dichloromethane solution. [b] Supporting electrolyte TBAP; reference electrode SCE; $E_{1/2} = 0.5$ ($E_{pa} + E_{pc}$), where E_{pa} and E_{pc} are anodic and cathodic peak potentials, respectively; $\Delta E_p = E_{pa} - E_{pc}$; scan rate 50 mV s^{-1}. [c] Shoulder. [d] E_{pc} value.

Table 4 EPR g-values[a] and derived parameters[b] of the [Ru(PPh$_3$)$_2$(L)Cl$_2$] complexes

Compound	g_1	g_2	g_3	Δ/λ	V/λ	$\Delta E_1/\lambda$	$\Delta E_2/\lambda$
[Ru(PPh$_3$)$_2$(L^1)Cl$_2$]	2.489	2.162	1.815	4.8060	3.4051	3.2603	6.7362
[Ru(PPh$_3$)$_2$(L^2)Cl$_2$]	2.443	2.183	1.841	4.9915	3.0288	3.6083	6.7317
[Ru(PPh$_3$)$_2$(L^3)Cl$_2$]	2.443	2.266	1.831	4.6053	1.7442	3.8219	5.7561

[a] In 1 : 1 dichloromethane–toluene solution at 77 K. [b] Spin–orbit coupling constant (λ) for complexed ruthenium(III) is *ca.* 1000 cm^{-1}.

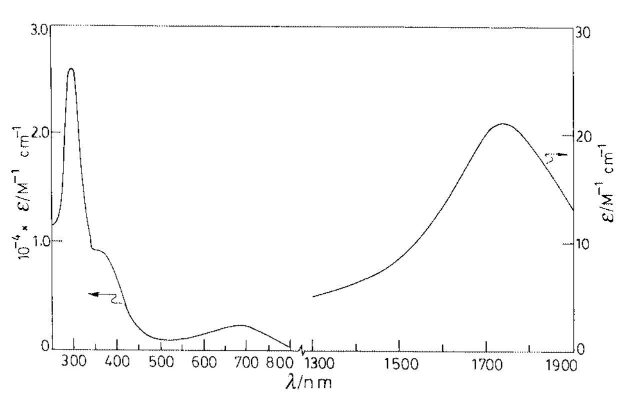

Fig. 2 Electronic spectrum of [Ru(PPh$_3$)$_2$(L^1)Cl$_2$] in dichloromethane solution.

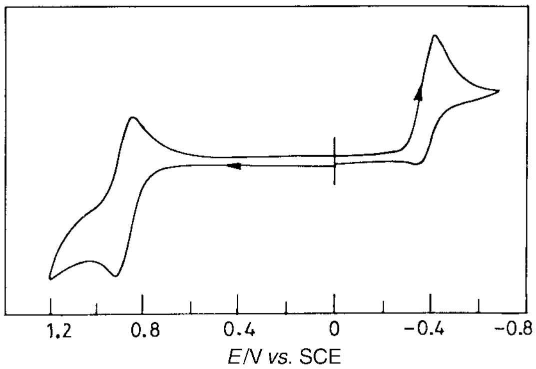

Fig. 4 Cyclic voltammograms of a 1.2 × 10^{-3} M solution of [Ru(PPh$_3$)$_2$(L^2)Cl$_2$] in dichloromethane (0.1 M TBAP) at a scan rate of 50 mV s^{-1}.

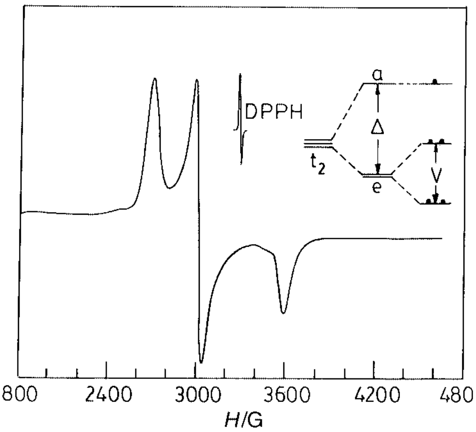

Fig. 3 EPR spectrum of [Ru(PPh$_3$)$_2$(L^3)Cl$_2$] in 1 : 1 dichloromethane–toluene solution at 77 K.

transitions. The origin of the weak absorption in the near-IR region is discussed below.

Magnetic susceptibility measurements show that the [Ru(PPh$_3$)$_2$(L)Cl$_2$] complexes are one-electron paramagnetic (Table 3), which corresponds to the trivalent state of ruthenium (low-spin d^5, $S = \frac{1}{2}$) in these complexes. Electron paramagnetic resonance (EPR) spectra of the [Ru(PPh$_3$)$_2$(L)Cl$_2$] complexes, recorded in 1 : 1 dichloromethane–toluene solution at 77 K, show rhombic spectra with three distinct signals (g_1, g_2 and g_3, in decreasing order of magnitude). A representative spectrum is shown in Fig. 3 and the spectral data are presented in Table 4. The observed rhombicity of the EPR spectra is understandable in terms of the gross molecular symmetry of these complexes, containing the three non-equivalent P–Ru–P, O–Ru–Cl and N–Ru–Cl axes. The rhombic distortion can be thought of as a combination of axial distortion (Δ, which splits t$_2$ into a and e) and rhombic distortion (V, which splits e). The splitting pattern is illustrated in Fig. 3. Spin–orbit coupling causes further changes in the energy gaps. Thus two electronic transitions (transition energies ΔE_1 and ΔE_2; $\Delta E_1 < \Delta E_2$) are possible within these three levels. All these energy parameters have been computed (Table 4) using the observed g-values, the g-tensor theory of low-spin d^5 complexes and a reported method.[12] The axial distortion is observed to be much stronger than the rhombic. The ΔE_1 transition falls in the infrared region (3200–3800 cm^{-1}) and could not be detected. The ΔE_2 transition, which is expected to occur near 6000 cm^{-1} (*ca.* 1667 nm), is indeed displayed by all three [Ru(PPh$_3$)$_2$(L)Cl$_2$] complexes as a weak absorption near the predicted energies (Tables 3 and 4). The EPR data analysis thus shows that the [Ru(PPh$_3$)$_2$(L)Cl$_2$] complexes are significantly distorted from ideal octahedral geometry, as observed in the crystal structure of [Ru(PPh$_3$)$_2$(L^2)Cl$_2$].

The electrochemical properties of the [Ru(PPh$_3$)$_2$(L)Cl$_2$] complexes have been studied in dichloromethane solution (0.1 M TBAP) by cyclic voltammetry. Voltammetric data are given in Table 3 and a representative voltammogram is displayed in Fig. 4. All three complexes show one oxidative response on the positive side of SCE and one reductive response on the negative side. The oxidation is assigned to ruthenium(III)–ruthenium(IV) oxidation. This oxidation is quasi-reversible in nature, characterized by a peak-to-peak separation (ΔE_p) of 70 mV, and the cathodic peak current (i_{pc}) is lower than the anodic peak current

(i_{pa}). The reductive response is irreversible and is assigned to ruthenium(III)–ruthenium(II) reduction. The one-electron nature of these responses has been confirmed by comparing their current heights with the standard ferrocene/ferrocenium couple under identical experimental conditions.

Conclusion

The present study shows an interesting oxo-transfer reaction mediated by [Ru(PPh$_3$)$_3$Cl$_2$]. The applicability of [Ru(PPh$_3$)$_3$Cl$_2$] as a mediator to bring about oxo-transfer reactions from various oxygen-containing ligands is currently under investigation. The reactivity of the *cis*-RuCl$_2$ fragment of the [Ru(PPh$_3$)$_3$(L)-Cl$_2$] complexes is also being explored.

Acknowledgements

Financial assistance received from the Council of Scientific and Industrial Research, New Delhi [Grant No. 01(1408)/96/EMR-II] is gratefully acknowledged. Thanks are also due to the Third World Academy of Sciences for financial support enabling the purchase of an electrochemical cell system.

References

1 C. Pearson and A. L. Beauchamp, *Inorg. Chem.*, 1998, **37**, 1242; T. Hashimoto, A. Endo, N. Nagao, G. P. Sato, K. Natrajan and K. Shimizu, *Inorg. Chem.*, 1998, **37**, 5211; P. Paul, B. Tyagi, A. K. Balikakhiya, M. M. Bhadbhade, E. Suresh and G. Ramachandraiah, *Inorg. Chem.*, 1998, **37**, 5733; J. Y. Lu, B. R. Cabrera, R. J. Wang and J. Li, *Inorg. Chem.*, 1998, **37**, 4480; E. V. Rybak-Akimova, A. Y. Nazarenko and S. S. Silchenko, *Inorg. Chem.*, 1999, **38**, 2974.

2 T. A. Stephenson and G. Wilkinson, *J. Inorg. Nucl. Chem.*, 1966, **28**, 945.

3 A. I. Vogel, *A Text Book of Practical Organic Chemistry*, ELBS, London, 1971, pp. 957–958.

4 (*a*) D. T. Sawyer and J. L. Roberts, Jr., *Experimental Electrochemistry for Chemists*, Wiley, New York, 1974, pp. 167–215; (*b*) M. Walter and L. Ramaley, *Anal. Chem.*, 1973, **45**, 165.

5 E. J. Gabe, Y. Le Page, J. P. Charland, F. L. Lee and P. S. White, *J. Appl. Crystallogr.*, 1989, **22**, 384.

6 S. Chattopadhyay, N. Bag, G. K. Lahiri and A. Chakravorty, *J. Chem. Soc.*, *Dalton Trans.*, 1990, 3389; S. Bhattacharya and C. G. Pierpont, *Inorg. Chem.*, 1991, **30**, 1511; M. Menon, A. Pramanik, N. Bag and A. Chakravorty, *J. Chem. Soc.*, *Dalton Trans.*, 1995, 1417.

7 K. Sui, S. M. Peng and S. Bhattacharya, *Polyhedron*, 1999, **18**, 631; F. Basuli, A. K. Das, G. Mostafa, S. M. Peng and S. Bhattacharya, submitted for publication.

8 B. A. Moyer, B. K. Sipe and T. J. Meyer, *Inorg. Chem.*, 1981, **20**, 1475; M. E. Marmoin and K. J. Takeuchi, *J. Am. Chem. Soc.*, 1988, **110**, 1472; C. M. Che and K. Y. Yong, *J. Chem. Soc.*, *Dalton Trans.*, 1989, 2065.

9 S. Bhattacharya and C. G. Pierpont, *Inorg. Chem.*, 1991, **30**, 2906; N. C. Pramanik and S. Bhattacharya, *Trans. Met. Chem.*, 1999, **24**, 95.

10 J. R. Dyer, *Application of Absorption Spectroscopy of Organic Compounds*, Prentice-Hall of India Pvt. Ltd., New Delhi, 1989, 37.

11 S. Choudhury, M. Kakoti, A. K. Dev and S. Goswami, *Polyhedron*, 1992, **11**, 3183.

12 B. Bleany and M. C. M. O'Brien, *Proc. Phys. Soc.*, *London*, *Sect. B*, 1956, **69**, 1216; J. S. Griffith, *The Theory of Transition Metal Ions*, Cambridge University Press, London, 1961, p. 364; S. Bhattacharya and A. Chakravorty, *Proc. Indian Acad. Sci.*, *Chem. Sci.*, 1985, **95**, 159.

Paper a907021d